TSINGHUA SCIENCE AND TECHNOLOGY
ISSN 1007-0214 01/18 pp495-500
Volume 11, Number 5, October 2006

A Modified Cellular Automaton Method for the Modeling of the Dendritic Morphology of Binary Alloys*

LIU Ying (刘 影), XU Qingyan (许庆彦)**, LIU Baicheng (柳百成)

Department of Mechanical Engineering, Tsinghua University, Beijing 100084, China

Abstract: A cellular automaton (CA)-based model for the precise two-dimensional simulation of the dendritic morphology of cast aluminum alloys was developed. Compared with previous CA models, the new model considers the solidification process in more detail, solving the solute and heat conservation equations in the modeling domain, including calculation of the solid fraction, the tip velocity, and the solute diffusion process, all of which have significant influence on the dendrite evolution. The rotating grids technique was used in the simulation to avoid anisotropy introduced by the square grid. Dendritic grain profiles for different crystallographic orientations show the existence of a great number of regular and parallel secondary and tertiary arms. The simulation results for the secondary arm spacing and grain size were compared with experimental data and with results reported in the literature. A good agreement was found between the simulated results and the experimental data. It can be concluded that the model can be used to predict the dendritic microstructure of aluminum alloy in a quantitative manner.

Key words: Al alloy; dendritic morphology; modified cellular automaton; grain size; secondary arm spacing

Introduction

The solidification microstructure of a casting is closely associated with the mechanical properties of the final product, which has led to extensive theoretical and experimental studies in this area. However, because of its complexity, the formation of a dendritic microstructure is not yet well understood and further research is required.

Experiments that allow direct visualization of dendrite growth phenomena in metals are difficult to perform due to the opacity and high melting point of metals[1,2]. In recent decades, several analytical models have been developed to calculate various microstructural features of a solidifying material, such as the solidification interface morphology transition, the dendrite tip velocity, and the primary and secondary dendrite arm spacing[3-5]. However, the complexity of dendrite formation and growth renders the problem difficult to address using analytical techniques. Consequently, only steady state cases have been studied in detail.

In order to overcome the limitations associated with analytical methods, computer simulation techniques have been exploited, and several models have been proposed. Among of them, the cellular automaton (CA) model and the phase field (PF) model are most popular and widely used. PF models can simulate the kinetics of dendritic growth by incorporating several factors that affect growth, such as crystallographic orientations and the motion of the boundaries during impingement[6,7]. The main limitations of the PF model are the

Received: 2005-01-26; revised: 2005-04-19

* Supported by the National Natural Science Foundation of China (No. 10477010) and the National Key Basic Research and Development (973) Program of China (No. G2000067208-3)

** To whom correspondence should be addressed.
E-mail: scjxqy@tsinghua.edu.cn; Tel: 86-10-62789922

complexity of the required calculations and the restricted simulation field, though some recent advances in the governing equations and in numerical techniques are helping to work around these limitations[8]. The CA model uses the concept of a diffuse interface and grid cells[9]. The states of the CA cells are governed by transition rules, which determine the behavior of each cell with respect to the state of the neighboring cells[10,11]. There are, however, some problems with existing models using the CA method that they cannot simulate the precise dendritic morphology, e.g., the secondary dendrites that take into account the influence of solute diffusion and also that artificial anisotropy associated with the square cells is introduced, which restricts significantly the way in which the interface moves[12,13].

The objective of the paper is to present a mathematical model for 2-D simulation of dendrite formation based on the traditional CA model. The new model attempts to obtain the precise dendritic morphology, including the secondary and tertiary arms by solving the solute and heat conservation equations at the interface and by considering other important factors, such as the solid fraction, the tip velocity, and the diffusion process of the solutes. The model also avoids artificial anisotropy by rotating the growth direction of the square cells to the preferential growth orientation.

1 Mathematical Model for Dendrite Formation

The mathematical model of the dendritic growth is considered in a restricted rectangle domain initially at a homogeneous temperature T_0 and composition C_0 as shown in Fig. 1. The solidification process of a binary aluminum alloy is governed by the evolution of the temperature field, the concentration field, and the velocity field. Note that a full list of all symbols used is given at the end of the paper.

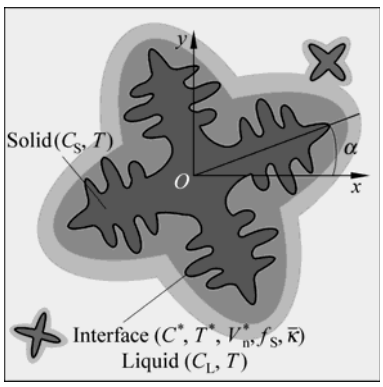

Fig. 1 Calculation domain of dendritic growth

1.1 Mathematical description of the solidification process

Heat transfer equation of the whole domain is

$$\rho c_p \frac{\partial T}{\partial t} = \lambda\left(\frac{\partial^2 T}{\partial x^2} + \frac{\partial^2 T}{\partial y^2}\right) - \rho L \frac{\partial f_L}{\partial t} \tag{1}$$

Solute conservation equation in the liquid phase is

$$\frac{\partial C_L}{\partial t} = D_L\left(\frac{\partial^2 C_L}{\partial x^2} + \frac{\partial^2 C_L}{\partial y^2}\right) - \left(V_x \frac{\partial C_L}{\partial x} + V_y \frac{\partial C_L}{\partial y}\right) \tag{2}$$

Solute conservation equation in the solid phase is

$$\frac{\partial C_S}{\partial t} = D_S\left(\frac{\partial^2 C_S}{\partial x^2} + \frac{\partial^2 C_S}{\partial y^2} + \frac{\partial^2 C_S}{\partial z^2}\right) \tag{3}$$

Solute conservation, local equilibrium, and temperature at the solid-liquid interface are

$$V_n^* C_L^* (1-k) = D_L\left(\frac{\partial C_L}{\partial x} + \frac{\partial C_L}{\partial y}\right) - D_S\left(\frac{\partial C_S}{\partial x} + \frac{\partial C_S}{\partial y}\right) \tag{4}$$

$$C_S^* = kC_L^* \tag{5}$$

$$T^* = T_L^{EQ} + (C_L^* - C_0)m_L - \Gamma\kappa f(\varphi,\theta) \tag{6}$$

1.2 Nucleation model

A continuous nucleation model based on Gaussian distribution of nucleation was used in the simulation to calculate the nucleation rate[14]. The nucleation model assumes that the grain density grows continuously with increasing undercooling. The density of new grains at a given undercooling is given as follows:

$$\frac{\mathrm{d}n}{\mathrm{d}(\Delta T)} = \frac{n_{\max}}{\sqrt{2\pi}\Delta T_\sigma}\exp\left[-\frac{(\Delta T - \Delta T_N)^2}{2(\Delta T_\sigma)^2}\right] \tag{7}$$

$$\delta n = \int_{\Delta T}^{\Delta T + \delta(\Delta T)} \frac{\mathrm{d}n}{\mathrm{d}(\Delta T)}\mathrm{d}(\Delta T) \tag{8}$$

After the number of new grains in each time step is calculated, the location of these new grains is chosen randomly from among the remaining liquid cells.

1.3 Cell capturing rules of the solidifying front

It is assumed that there exist three kinds of possible cells, i.e., liquid, solid, and interface cells, in the simu-

lation domain, as shown in Fig. 2. At the beginning of solidification, all cells are liquid. When the temperature falls below the liquidus, some liquid cells will become interface cells (and later solid cells) as nucleation and grain growth proceeds. The capturing rules are defined as: (1) When nucleation takes place in a liquid cell, or a liquid cell is captured by a solid one, it becomes an interface cell; (2) When an interface cell grows with the velocities V_x and V_y, which can be obtained from Eq. (4), the solid fraction increment is calculated as follows:

$$\partial f_{\mathrm{S}} = \frac{\delta t}{a}(V_x + V_y - V_x V_y \frac{\delta t}{a}) \tag{9}$$

(3) When f_{S}=1, the interface cell becomes solid. At such a time, the solid cell can capture its four neighbor cells and convert them into interface cells if a randomly generated real number, rand, is smaller than the capturing probability, p_{c}, defined as follows:

$$p_{\mathrm{c}} = \frac{1}{\sqrt{1+\tan^2\theta}} \tag{10}$$

The capturing process is shown in Fig. 2, where the demonstration interface cell is marked in black, and its four neighbor cells are marked in black dots. The above procedures are repeated again and again until all cells are converted to solid state.

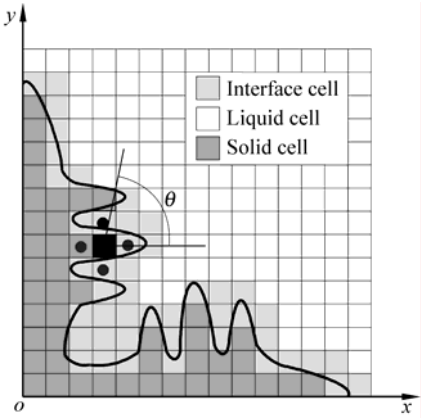

Fig. 2 Capturing rules during the advance of interface cells

1.4 Grids rotating technique

In previous CA models, the grid anisotropy is always a problem in that whatever crystallographic growth orientation is assigned first to a dendrite, the final dendrite orientation always shifts towards 0° as solidification proceeds because the calculating domain is divided into horizontal and vertical rectangles. In this paper, the grid cell direction is adjusted to coincide with the crystallographic growth orientation by rotating the grid and using a coordinate transformation, as shown in Fig. 3.

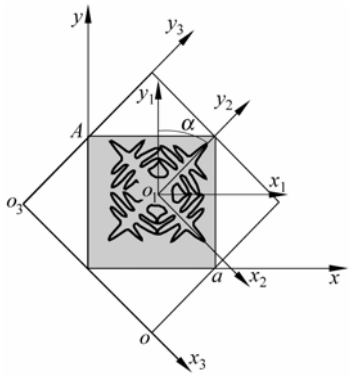

Fig. 3 The principle of the coordinate transformation during the dendritic grain growth

The nuclear point is assumed to be (x_0, y_0) and the calculation domain of size a is shown in gray. The rotation process follows the steps: (1) translate the origin of the xoy coordinate system to the point (x_0, y_0) (the center of the dendrite); (2) rotate the $x_1o_1y_1$ coordinate system by the orientation angle α; (3) translate the $x_2o_1y_2$ coordinate system to the $x_3o_3y_3$ system through the points "o" and "a" and set up grids whose axis directions are the preferred directions; (4) mark the grids in the $x_3o_3y_3$ system that the gray calculation domain covers; (5) calculate the results in the $x_3o_3y_3$ system, and then translate the coordinates from the $x_3o_3y_3$ to the xoy system using the following equations

$$x = x_0 + \left[x_3 - (a - y_0)\sin\alpha - x_0\cos\alpha\right]\cos\alpha + \left[y_3 - (y_0\cos\alpha + x_0\sin\alpha)\right]\sin\alpha \tag{11}$$

$$y = y_0 + \left[y_3 - (y_0\cos\alpha + x_0\sin\alpha)\right]\cos\alpha - \left[x_3 - (a - y_0)\sin\alpha - x_0\cos\alpha\right]\sin\alpha \tag{12}$$

2 Simulation Results and Discussion

The thermophysical properties of the Al-4.5wt.%Cu alloy used for the simulations are presented in Table 1. Simulation of single equiaxed grain growth with various crystallographic orientations using the rotating grids method was performed for an Al-4.5wt.%Cu alloy in a square domain, as shown in Fig. 4. It is assumed that the initial temperature and concentration of liquid is uniform in the calculated region, which was

divided into 500×500 cells with grid size $\delta x=\delta y=1$ μm. It can be seen that the grain envelopes shown in Figs. 4a-4c are similar to the experimental results, shown in Fig. 4d, and that the secondary dendritic arms are parallel with each other and normal to the primary dendritic stems. The lowest and highest chemical composition lie, respectively, in and between the dendritic stems and the solute concentration decreases from the dendritic interface to the liquid phase, as can be seen by the change in colors in Figs. 4a-4c. The results are consistent with those from a theoretical analysis.

Table 1 Thermophysical data used in the simulations

Parameter	Value
L / (J • kg^{-1})	3.97×10^{5}
ρ / (kg • m^{-3})	2550
K/ (W • m^{-1} • K^{-1})	90
C_p/(J • kg^{-1} • K^{-1})	1100
T_L/ ℃	641
C_0/ (wt.%)	4.5
k_0	0.14
D_S/ (m^2 • s^{-1})	3×10^{-9}
D_L/ (m^2 • s^{-1})	1×10^{-12}
m_L/ (℃ • wt.%$^{-1}$)	−6.5
Γ/(K • m)	0.9×10^{-7}

Figures 5a and 5c show micrographs of Al-4.5wt.%Cu casts using sand and metal molds, respectively. The grain contours can be seen clearly. The corresponding modeling results using the above models and algorithm are shown in Figs. 5b and 5d. It can be seen that the modeled grain contours and grain sizes are similar to the experimental micrographs. The cooling speed is lower for a sand mold compared to a metal mold; hence the nucleation rate is smaller and the grain size is larger for sand mold casting.

Figure 6 shows the simulated growth and selection of secondary dendrite arms for a Al-4.5wt.%Cu alloy under similar conditions to those mentioned in Ref. [15]. The calculation domain was rectangular with grid size $\delta x=\delta y=1$ μm and 400×100 cells. Periodic conditions to the right and left lateral sides are used in the simulation and the other two boundaries are insulated. The temperature of the whole domain was reduced uniformly from the liquidus temperature. Nucleus appeared only at the left corner of rectangular domains from where the growth began. In Fig. 6, the solidification process, including nucleus generation, grain growth, coarsening, selection of the secondary arms,

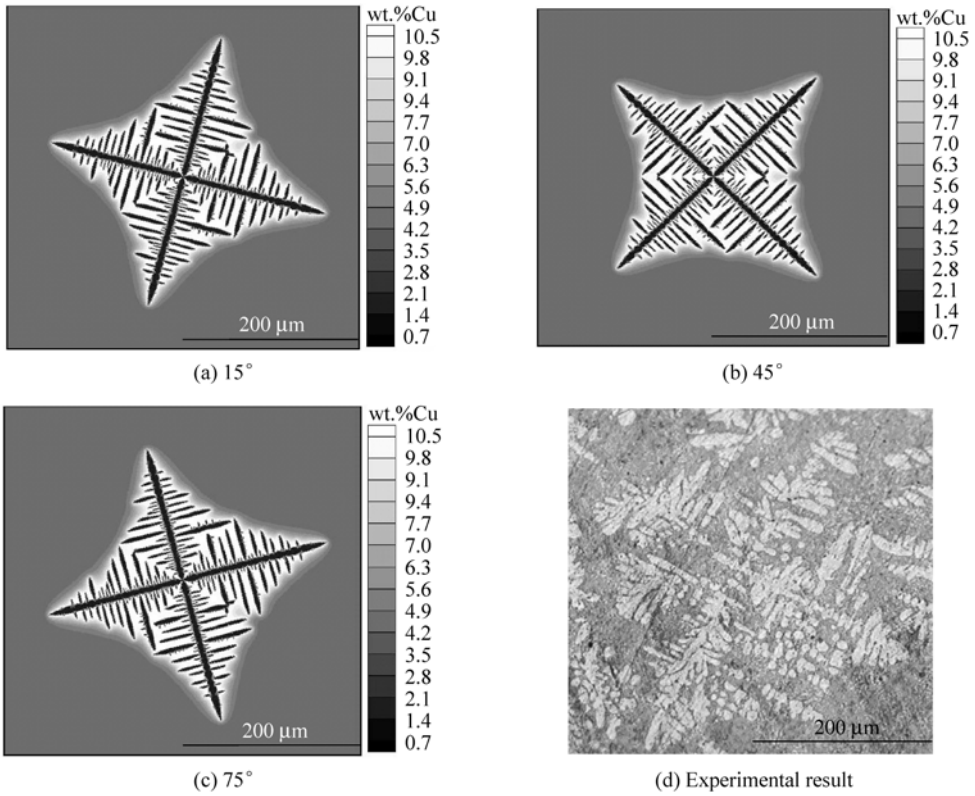

Fig. 4 Single equiaxed grain growth with different preferential orientations

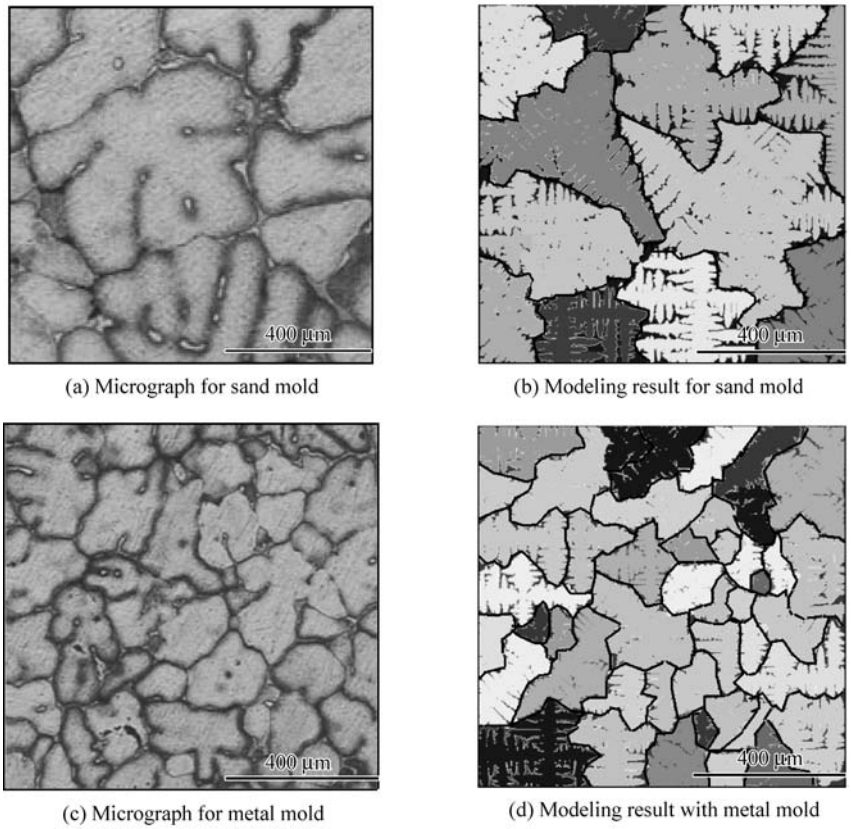

Fig. 5 Comparison of grain contours between modeling results and experimental micrographs

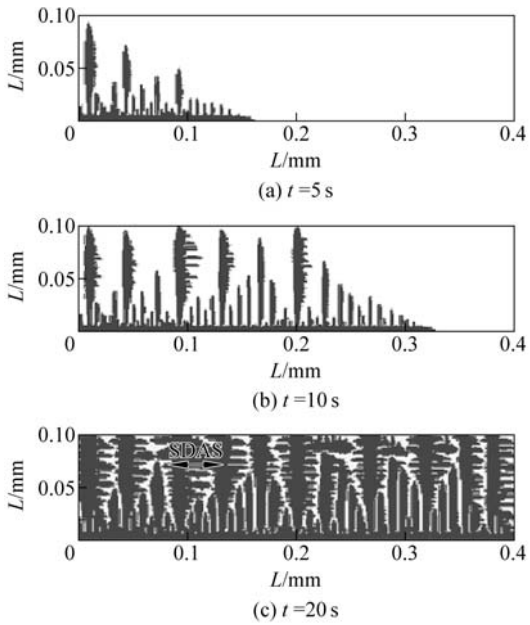

Fig. 6 The growth and selection of secondary dendrite arms for Al-4.5wt.%Cu alloy

and the appearance of tertiary branches, can all be seen clearly. An average value for the spacing of the secondary arms (SDAS) was calculated at the end of solidification. Figure 7 shows a comparison of the simulated SDAS data with results from the literature for a series of local solidification times. The simulated results correspond well with the results from the literature.

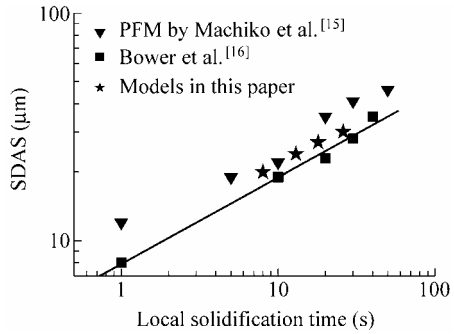

Fig. 7 Relationship between SDAS and local solidification time

3 Conclusions

A CA-based model for the precise two-dimensional simulation of dendritic morphology of aluminum alloys was developed by solving solute and heat

conservation equations at the interface including the calculation of the solid fraction, the tip velocity, and the diffusion solute process. Other factors such as constitutional undercooling, curvature undercooling, and growth anisotropy, all of which have a critical influence on the dendrite evolution, were also considered. Simulation results show that this model is able to reproduce most of the dendritic features observed experimentally, such as secondary and tertiary branching, arm generation, selection, and coarsening. The calculated results for secondary dendritic arm spacing and grain size were similar to both experimental measurements and to values reported in the literature. It can be concluded that the model can be used to predict the dendritic microstructure of aluminum alloy in a quantitative manner.

Acknowledgements

One of the authors, Dr. Xu Qingyan, would like to thank the Key Lab Open Research Fund from Lanzhou University of Technology.

Nomenclatures

c_p	Specific heat, J • kg^{-1} • K^{-1}
C_L^*	Liquid species mass fraction at interface, %
C_S^*	Solid species mass fraction at interface, %
C_0	Initial species mass fraction, %
C_L	Species mass fraction in liquid, %
C_S	Species mass fraction in solid, %
D_L	Species diffusion coefficient in liquid, m^2 • s^{-1}
D_S	Species diffusion coefficient in solid, m^2 • s^{-1}
f_L	Mass fraction of liquid
$f(\varphi,\theta)$	Anisotropy of surface tension
k	Equilibrium partition ratio
L	Latent heat, J • kg^{-1}
m_L	Liquidus slope, ℃/%
n_{max}	Maximum density of grain, m^{-3}
ΔT	Temperature of undercooling, K
ΔT_σ	Standard deviation of temperature distribution, K
ΔT_N	Temperature of centre of distribution, K
T^*	Interface temperature, K
T_L^{EQ}	Liquidus temperature, K
V_x, V_y	Component of velocity, m • s^{-1}
V_n	Interface moving velocity, m • s^{-1}
λ	Thermal conductivity, W • m^{-1} • K^{-1}
ρ	Density, kg/m^3
Γ	Gibbs-Thomson coefficient, m • K
κ	Curvature of interface, m^{-1}
θ	Angle between normal and preferential growth orientation

References

[1] Glicksman M E, Winsa E, Hahn R C, Lograsso T A. Isothermal denritic growth – A proposed microgravity experiment. *Metall. Trans.*, 1988, **19A**: 1945-1953.

[2] Chopra M A, Glicksman M E, Singh N B. Equiaxed dendrite growth in alloys at small supercooling. *Metall. Trans*., 1987, **18A**: 341-345.

[3] Trivedi R, Kurz W. Dendritic growth. *Int. Mater. Res.*, 1994, **9**(2): 49-74.

[4] Lipton J, Glicksman M E, Kurz W. Dendritic growth into undercooled alloy melts. *Mater. Sci. Eng.*, 1984, **65**: 57-63.

[5] Langer J S, Müller-K H. Theory of dendritic growth I. Elements of a stability analysis. *Acta Metall.*, 1978, **26**: 1681-1687.

[6] Nestler B, Wheeler A A. Anisotropic multi-phase-field model: Interfaces and junctions. *Phys. Rev. E*, 1998, **57**(3): 2603-2609.

[7] Warren J A, Kobayashi R, Carter W C. Modeling grain boundaries using a phase-field technique. *Journal of Crystal Growth,* 2000, **211**: 18-20.

[8] Karma A, Rappel W J. Quantitative phase-field modeling of dendritic growth in two and three dimensions. *Phys. Rev. E*, 1998, **E57**: 4323-4349.

[9] Charbon Ch, Rappaz M. A coupled finite element-cellular automaton model for the prediction of dendritic grain structures in solidification. *Acta Metall.*, 1994, **42**(7): 2233-2246.

[10] Nastac L. Numerical modeling of solidification morphologies and segregation patterns in casting dendritic alloys. *Acta Metall.*, 1999, **47**(17): 4253-4262.

[11] Xu Q Y, Feng W M, Liu B C. Stochastic modeling of dendritic microstructure of aluminum alloy. *International Journal of Cast Metals Research*, 2002, **15**(3): 225-230.

[12] Gandin Ch-A, Rappaz M. A 3D cellular automaton algorithm for the prediction of dendrtic grain growth. *Acta Mater*., 1997, **45**(5): 2187-2195.

[13] Beltran S L, Stefanescu D M. Growth of solutal dendrites-a cellular automaton model. *International Journal of Cast Metals Research*, 2002, **15**(3): 251-256.

[14] Thévoz Ph, Kesbiollex J L, Rappaz M. Modeling of equiaxed microstructure formation in casting. *Metall. Trans*.**,** 1989, **20A**: 311-322.

[15] Machiko O, Seong G K, Won T K, Toshio S. Numerical prediction of secondary dendrite arm spacing using a phase-field model. In: The Science of Casting and Solidification. Lux Libris, Brasov, Romania, 2001: 139-140.

[16] Bower T F, Brody H D, Flemings M C. Measurements of solute redistribution in dendritic solidification. *Transaction of Metallurgical Society of AIME*, 1996, **236**: 624-634.